

Hysteretic Optimization For Spin Glasses

B. Gonçalves and S. Boettcher
Emory University, Atlanta, Ga 30322*

The recently proposed Hysteretic Optimization (HO) procedure is applied to the 1D Ising spin chain with long range interactions. To study its effectiveness, the quality of ground state energies found as a function of the distance dependence exponent, σ , is assessed. It is found that the transition from an infinite-range to a long-range interaction at $\sigma = 0.5$ is accompanied by a sharp decrease in the performance. The transition is signaled by a change in the scaling behavior of the average avalanche size observed during the hysteresis process. This indicates that HO requires the system to be infinite-range, with a high degree of interconnectivity between variables leading to large avalanches, in order to function properly. An analysis of the way auto-correlations evolve during the optimization procedure confirm that the search of phase space is less efficient, with the system becoming effectively stuck in suboptimal configurations much earlier. These observations explain the poor performance that HO obtained for the Edwards-Anderson spin glass on finite-dimensional lattices, and suggest that its usefulness might be limited in many combinatorial optimization problems.

I. INTRODUCTION

The steadily increasing availability of powerful computational resources has allowed scientists and engineers alike to study ever more realistic and complex problems. Historically, a significant fraction of all available computer time has been used to traverse phase space in search of the optimal solution to a given problem.

Particularly, in several physics domains[1], such as spin glasses, disordered materials and protein folding, one is interested in enumerating a large number of local minima of the energy landscape [2, 3], as that provides us with valuable information about its physical properties. Many algorithms and heuristics have been developed over the years to tackle this kind of problem. In this article we study a recently proposed algorithm known as Hysteretic Optimization (HO)[4–7]. HO is motivated by the physics of demagnetizing magnetic materials with a slowly oscillating external field of decreasing amplitude. Similar to the thermal fluctuations in simulated annealing [8] or the activated dynamics of extremal optimization (EO) [9], the drag created by the external field carries HO over energetic barriers.

HO has proved efficient[6] at finding the ground state configurations of the well known Sherrington-Kirkpatrick (SK)[10] mean-field spin glass and of the classical Traveling Salesman Problem, but has, hitherto, been unsuccessful in searching the corresponding Edwards-Anderson spin glass on finite-dimensional lattices[11], as described in Chap. 10 of Ref. [1]. Similarly, it was shown in Ref. [12] that HO performs poorly for the random field Ising model (RFIM) on a one or three dimensional lattice. (The RFIM is a classic model for disordered magnetic materials, but unlike the spin glass case there are polynomial-time algorithms to find global optima in the energy landscape, see Chap. 5 in Ref. [1].) Since efficient heuristics for hard (i. e. beyond polynomial) optimiza-

tion problems are still few and far between, especially for spin glasses, but also for many other combinatorial problems[13], promising new algorithms warrant careful investigation. Here, we explore the behavior of HO under variation of the search space characteristics that is representative of many problems. In particular, we apply HO to a one-parameter family of spin glass problems [14–18] that interpolates between the characteristics of the SK model on one extreme and the EA model on the other. We observe that the break-down of HO for the EA model is intimately linked to the physics of intermittent events (i. e. avalanches) kicked-off by the external field in the hysteresis loop. We find a distinct cross-over between broadly-distributed avalanching dynamics in the SK-regime[19], connected with a high degree of interconnectivity between variables and divergent energy scales, and sharply cut-off dynamics in the EA regime. Unfortunately, the need for strong interconnectivity between variables severely limits the applicability of HO with respect to combinatorial problems related to spin glasses of low degree such as satisfiability, partitioning, or coloring at their respective phase transitions [13].

This article is structured as follows, in Section II, we introduce the general Hysteretic Optimization procedure and apply it to a generalization spin glass model. In Section III, we investigate in detail the avalanche dynamics during the hysteresis process to identify the reasons that lead to the breakdown of HO's performance.

II. HYSTERETIC OPTIMIZATION

For a magnetic material, such as an Ising system, to obtain a zero magnetization value, an a.c. demagnetization is performed. The sample is placed in an oscillating and slowly decaying magnetic field. As the amplitude of the external field approaches zero, so does the magnetization. At low enough temperature and slow driving, a disordered systems gets dragged through a sequence of local energy minima. Based on this observation, Zaránd *et al* [4] proposed Hysteretic Optimization (HO) as a general-

*Electronic address: bgoncalves@physics.emory.edu

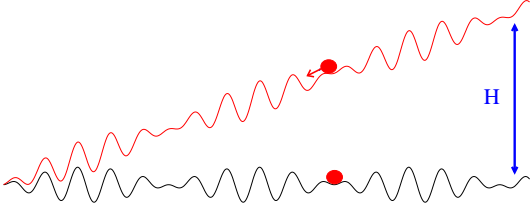


Figure 1: Simple sketch of a one-dimensional slice through the energy landscape for a generic optimization problem as in Eq. (1) without external field (bottom) and in Eq. (2) with external field (top).

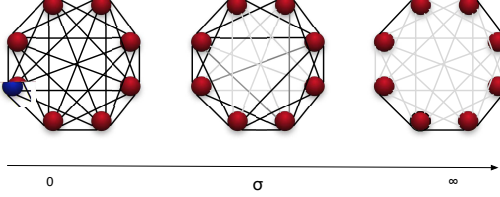


Figure 2: Systems described by the long-range spin glass model as a function of σ . For $\sigma \equiv 0$ we re-obtain the *SK* model and as $\sigma \rightarrow \infty$ all the long range links become essentially negligible leaving us only with nearest-neighbor interactions.

purpose local search heuristic[20] to explore the phase space of many combinatorial optimization problems. As an example, their study implemented the HO algorithm as listed in Tab. 1

Our study here is focused only on finding the ground state ($T = 0$) energies of spin glasses, for which case we describe the implementation of HO in detail.

In an Ising spin glass, each spin $S_i \in \{\pm 1\}$ is assumed to have a random bond $J_{i,j}$ with other spins S_j :

$$\mathcal{H} = - \sum_{\langle i,j \rangle} J_{ij} S_i S_j, \quad (1)$$

where the summation is taken over all pairs of spins. To find ground states of this spin glass with HO, we couple each spin σ_i to an external field of amplitude H . with a random sign $\xi_i \in \{\pm 1\}$, which may be adjusted even during a single demagnetization run. The Hamiltonian of this extended system is then:

$$\mathcal{H}_{HO} = \mathcal{H} + H \sum_i \xi_i S_i \quad (2)$$

Physically, the second term in Eq. (2) distorts the energy landscape as shown in Fig. 1, allowing the system to escape local minima. Fluctuations due to the coupling to the external field can compensate for unsatisfied bonds. By varying the external field H and the random couplings ξ_i , HO can force the system to explore a vast area of phase space in search of the optimal solution.

Algorithm 1 Hysteretic Optimization

1. Set $H = H_1$ large enough such that $S_i = \xi_i \forall i$. Set $E_{\{\min\}} = \mathcal{H} (= \mathcal{H}_{HO}|_{H=0})$.
 2. Decrease H until one spin becomes unstable and allow the system to relax. If $\mathcal{H} < E_{\{\min\}}$, set $E_{\{\min\}} = \mathcal{H}$.
 3. Optional: When H passes zero, randomize ξ_i , leaving the current configuration stable.
 4. At each turning point $H = H_n = -\gamma_{n-1} H_{n-1}$, for $0 < \gamma_n < 1$, reverse the direction of H .
 5. Terminate when amplitude $|H_n| < H_{\{\min\}}$.
 6. Restart at 1 for N_{run} times with a new, random set of ξ_i 's.
 7. Return the best $E_{\{\min\}}$ over all runs.
-

Following the prescription of Algorithm 1 for the variation of the external field H , each run, in effect, starts by exploring a large region of phase space which subsequently decreases slowly. By varying the field between positive and negative amplitudes $H_n = -\gamma_{n-1} H_{n-1}$, the runs repeatedly quench the system, following an approach similar to the well known simulated annealing or tempering algorithms[8, 21, 22].

HO operates at $T = 0$, thus there are no thermal fluctuations and we can simply calculate the field necessary to make the next spin unstable and increase it to that value (within the $\gamma^n H_0$ limit). Typically, HO is run with multiple restarts from the largest amplitude to increase the chances of finding a better approximation to the global minimum. Note, however, that each run itself has no stochastic element once the couplings ξ_i to the external field are fixed. It is therefore useful to restart the demagnetization process repeatedly with a fresh set of random field directions (see item 6. in Algorithm 1). In fact, it is also possible to refresh the ξ_i each time the external field H passes through zero during each run (see item 3 in Alg. 1).

This algorithm has been very successful in determining the ground state energies of the Sherrington-Kirkpatrick spin glass[6] and reasonably efficient for the Traveling Salesman Problem[23], but there are few attempts to apply it to other problems[12]. In this article we focus on a Ising spin glass on a one-dimensional ring with power-law interactions[14–18] defined by the Hamiltonian in Eq. (2) with bonds of the form:

$$J_{i,j} = \frac{\epsilon_{ij}}{r_{ij}^\sigma}. \quad (3)$$

Here, ϵ_{ij} are random variables drawn independently from a Gaussian distribution of zero mean and unit variance and

$$r_{ij} = \frac{L}{\pi} \sin\left(\frac{\pi|i-j|}{L}\right)$$

is the distance between each pair of spins on the ring. By varying σ we can interpolate between the all-to-all *SK*

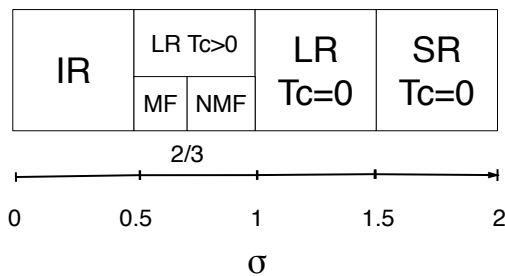


Figure 3: Phase diagram, after [14–18].

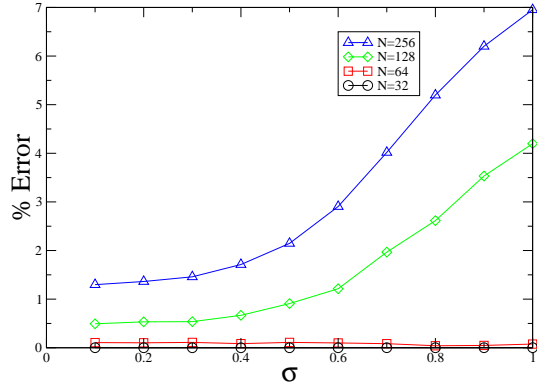


Figure 4: Percentage difference between the ground state found by Hysteretic Optimization and the one found by Extremal Optimization.

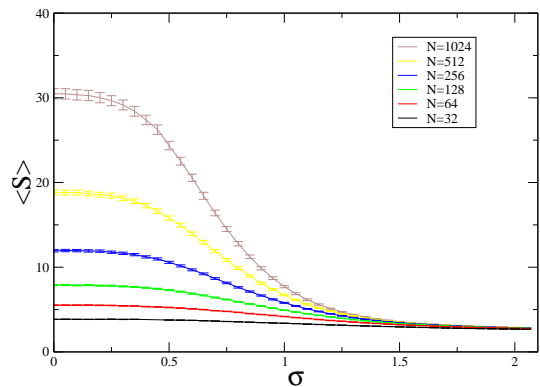
limit ($\sigma = 0$) and the nearest-neighbor *EA* limit (large σ), as shown in Fig. 2. This model has been extremely useful in elucidating the connection between mean-field and finite-dimensional spin glasses[17, 18].

As it has been shown in the literature [14, 24, 25], as σ is increased this spin glass goes through several distinct phases, see Fig. 3. For $0 \leq \sigma < 0.5$ the system is effectively Infinite Range (IR). For all σ , the singular part of the mean field transition temperature, T_c^{MF} , is of the order [17].:

$$(T_c^{MF})^2 \propto \sum_{i=2}^N [J_{i1}^2]_{av} = \sum_{i=2}^N r_{i1}^{-2\sigma} \sim N^{-2\sigma+1}$$

where $[\cdot]_{av}$ denotes an average over disorder with $[\epsilon_{ij}^2]_{av} = 1$. This temperature becomes finite in the thermodynamic limit at $\sigma = 0.5$, signaling a transition to a Long Range (LR) regime, where each node is able to see only a finite fraction of the rest of the system. At $\sigma = 1.0$, T_c becomes zero, but the LR character is preserved until $\sigma = 1.5$. From this point on, the structure of the system is purely Short Range (SR), and each spin is connected only to $O(1)$ neighbors

We have performed a benchmark study of the performance of *HO* on this spin glass model over a range of σ -values. The point of this study is not so much to tweak *HO* for optimal performance, but to obtain a

Figure 5: Average avalanche size as a function of σ for different system sizes.

clear assessment of its behavior under variation of this parameter. To this end, we generated a benchmark of instances of system sizes $N = 32, 64, 128$, and 256 , for which we have obtained extremely good approximation to the ground state energy by alternate means. In this case, we have used the Extremal Optimization heuristic (*EO*) [9, 26, 27] but expanding a large amount of CPU time to ensure accuracy. In fact, using the implementation described in Ref. [9], *EO* has proven itself equally capable of approximating ground states in the SK model[27] as for the *EA*[9], and it appears to be much less dependent on σ . Although a direct comparison is not justified here due to the disproportionate run times used for *EO*, we have found that even at much more extensive runs, *HO* was not able to find the exact-known ground state of a one-dimensional spin glass with more than $\approx 10^2$ spins[12].) In this set of instances, we have applied *HO* with a minimal set of control parameters. We set $\gamma = 0.99$ and for each instance in our set, we performed 10 different runs, each with a separate sets of ξ_i that were kept constant throughout the entire run. The ground state energy was taken to be the best value seen over 10 different quenches. This value was then averaged over 1000 different instances and compared with the results obtained by *EO* for *exactly* the same set of instances.

In Fig. 4 we plot the quality of the solution obtained by *HO* as a function of σ . The “Error” is defined as the percentage difference in ground state energy of the solutions found using *HO* relative to *EO*. Generally, the quality of the results found by *HO* diminishes for increasing system size for all σ , as can be expected with the limited CPU time (linear in N) apportioned to these runs. More noticeable is the ever more pronounced rise in error for $\sigma > 0.5$. To understand the physical reasons behind this behavior, we proceed to studying the dynamics of the system in the next section.

III. AVALANCHES AND CORRELATIONS

Unlike the comparison in the previous section, we now focus exclusively on the intrinsic behavior of HO itself. We will pinpoint the causes of HO s breakdown using quantitative measures. Using essentially the same program as previously, for each value of N , we perform 2 (undamped) hysteresis cycles each, but for a much larger set of $4 \cdot 10^4 \cdot \sqrt{32/N}$ instances. Throughout, we set $\xi \equiv 1$.

When the hysteresis procedure described causes a spin to become unstable and get flipped, this may cause several other spins to become unstable, thus initiating an avalanche in the system. Each avalanche can involve a significant fraction of the number of spins in the system, including, on occasion, several flips of the same spin in a form of long-range self interaction. Avalanches have a wide range of sizes and can, in principle, be larger than the system size by flipping the same spin multiple times.

As a first step in our analysis, we measure $\langle S(\sigma) \rangle$, the average avalanche size as a function of σ at different system sizes. This measurement will help us determine what range of σ we need to study, since it should become system size independent in the nearest-neighbor limit. As we show on the right hand side of Fig. 5, this happens near $\sigma \approx 2.0$, thus restricting our interval of interest to $\sigma \in [0, 2]$, as expected from the literature[17].

We find that this quantity obeys an empirical scaling relation of the form:

$$\langle S(N, \sigma) \rangle \sim \frac{NA(\sigma)f(N, \sigma) + B(\sigma)}{\log^2(N)} \quad (4)$$

where $A(\sigma)$, $B(\sigma)$ are linear functions of σ , and $f(N, \sigma)$ is plotted in Fig. 6. The overlap of all the curves in the interval $\sigma \in [0, 0.5]$ means that all the N dependence has been captured by the $N/\log^2(N)$ term. This scaling should be compared with the $N/\log(N)$ scaling found for this behavior for $\sigma = 0$, i. e. the SK model, by Ref. [19]. In fact, the emergence of log-corrections makes any definite determination of scaling behavior impossible over the range of system sizes N accessible here, and any of the following scaling relations should be viewed as purely phenomenological.

The scaling becomes increasingly worse with $\sigma > 0.5$, signaling a new N dependence.

We believe this change in behavior at $\sigma = 0.5$ is due to the topological change, from IR to LR, that occurs at this point (see the discussion in the previous section). Even though each node in the LR regime is still connected to other spins at arbitrarily large distances, its possible influence is now limited to a fraction of the total number of variables in the system, resulting in smaller avalanches. The avalanche size effectively creates a limit on the length of the jumps in configuration space that the system is capable of performing, forcing a less than optimal sampling of phase space, and increasingly poorer results.

Avalanche sizes are determined by the total number of spin flips that occur. If the same spin happens to flip

several times, then it will be counted multiple times as well, but we can also count the number U of just which spins flip at least once. The ratio S/U of the avalanche size, S , over the number of unique spins flipped, U , gives us a measure of how important loops are in the dynamics of the system, a large ratio will indicate that perturbations spread throughout the system and keep returning to the same spin, while a number close to unity would mean that avalanches propagate in just one direction and never double back.

On Fig. 7 we plot $\langle S/U(\sigma) - 1 \rangle$ for different system sizes. We find that the ratio between the size of the avalanche and the number of unique spins flipped is always small and becomes approximately system size independent in the Short Range phase. This confirms, once again, that in this region the sphere of influence of each spin is very small, being limited practically only to Near-est Neighbors.

This quantity obeys a phenomenological scaling relation of the form:

$$\left\langle \frac{S}{U}(N, \sigma) - 1 \right\rangle = \sqrt{N} [g(N, \sigma) - A \log(N)] \quad (5)$$

where $A \approx 4 \times 10^{-4}$ is a small constant and $g(N, \sigma)$ is shown in Fig. 8. The scaling collapse of the data is very good up to near $\sigma \approx 1.5$ where the system acquires a purely short range behavior. [Clearly, this collapse is purely phenomenological, as the log-correction in Eq. (5) would ultimately overwhelm the constant term.]

Finally, we study how the algorithm approaches the final configuration, at $H \approx 0$ and $m = 0$, by looking at the auto-correlation function given by:

$$\langle S_i^0 S_i^\tau \rangle - \langle S_i^0 \rangle \langle S_i^\tau \rangle \quad (6)$$

where the indices denote summation over all spins i . In Eq. (6), we measure the overlap between the final configuration and those obtained a number of τ complete cycles backwards in the past at their $H = 0$ -crossing. Intuitively, we expect that the configurations seen at the beginning of the procedure (large values of τ) will be

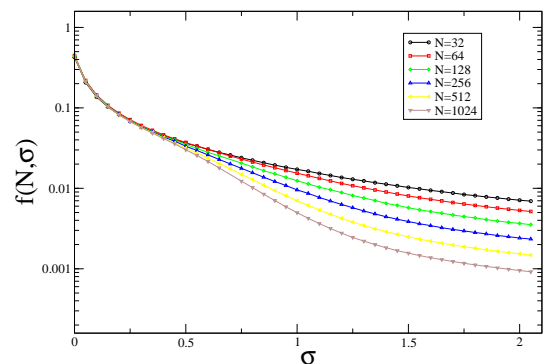


Figure 6: Corrections to scaling of the average avalanche size, rescaled according to Eq. (4).

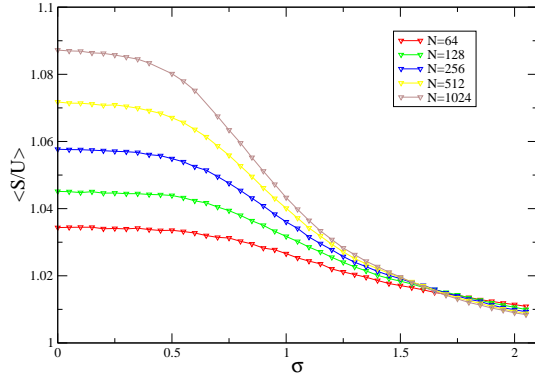


Figure 7: Ratio between the avalanche size and the number of spins that were flipped.

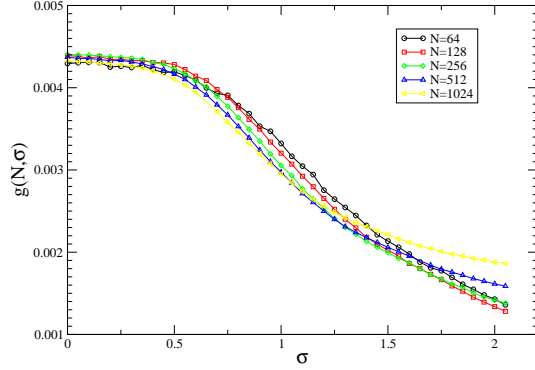


Figure 8: Scaling function $g(N, \sigma)$, as defined in Eq. (5).

completely unrelated to the final configuration ($\tau = 0$), resulting in a value near zero for this quantity. However, as the algorithm takes its course and approaches its conclusion, so too must the configurations start approaching the final one, corresponding to a value close to 1. The way in which it varies from values near 0 to values close to 1 gives us information about the way exploration of configuration space occurs. The longer the period during which the correlations are close to 0, the larger the volume explored, and the faster it gets close to zero, the earlier the system restricts itself to a given region, thus limiting the quality of the solution it is able to find.

In Fig. 9 we plot this quantity for the case of $N = 256$, averaged over 1000 different instances for each value of σ and with 10 different runs per instance. For small values of σ , the plateau at low correlations is extended (lower solid black curve), followed by an increase towards the value of 1 near the final stages $\tau \rightarrow 0$. As σ increases, the auto-correlations increase within the plateau which itself shortens, and the tendency towards 1 becomes noticeable right from the onset (upper solid red curve for $\sigma = 2$). This is a clear demonstration of the ideas expressed earlier, that the volume of configuration space explored becomes smaller with the decrease in avalanche size corresponding to increasing σ .

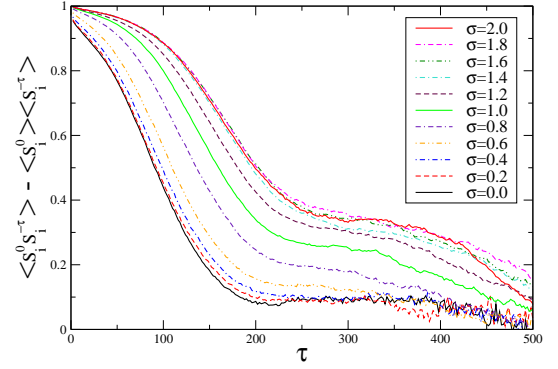


Figure 9: Correlation with the final solution as a function of the time in the past.

IV. DISCUSSION

The performance of the Hysteretic Optimization procedure for spin glasses was analyzed for a spin glass model that interpolates between systems with highly connected variables in the mean field limit and sparsely connected variables in the nearest-neighbor lattice limit. *HO* is shown to be very fast, but the quality of its solutions quickly start decaying for increasing values of the distance dependence exponent, σ . An analysis of the avalanche dynamics occurring in these systems revealed that the failure of *HO* is due to the truncation of avalanche size, and hence a limited exploration of the energy landscape, that occurs when the system is no longer in the Infinite Range phase.

The analysis of the behavior of the auto-correlation function with σ confirmed this idea by showing that *HO* becomes stuck in a limited region of configuration space increasingly earlier for larger values of the distance dependence exponent, σ .

HO, being dependent on avalanches for its local search, cannot continue to work when the avalanches are no longer large enough to facilitate large jumps in configuration space. Any attempt to use *HO* in a finite connected system, such as an Edwards-Anderson spin glass or many combinatorial optimization problems[13], is, therefore, inefficient (see Chap. 10 in Ref. [1] and Ref. [12]). Our attempts to simulate sparsely connected systems, in this case 3SAT[13] and EA spin glasses with $\pm J$ -bonds, with *discrete* bond weights proved particularly unsuccessful. In such system, all variables only possess a finite (and typically, small) range of local field states to take on. For instance, in such an EA spin glass in $d = 3$ dimensions, all spins have exactly $2d + 1 = 7$ states. Thus, a hysteresis loop has just 7 jumps between full up- and and full-down saturation. At each jump, a finite fraction of spins flip simultaneously due to degeneracies, but mostly in an *uncorrelated* manner dictated by their local environment. An open question remains that concerns problems defined on random graphs of finite connectivity but with a continuous distribution of bond-weights, such as the Viana-

Bray spin glass[28] with a Gaussian bond distribution. Unlike for a lattice, the number of neighbors increases exponentially with distance so that every node is connected to every other node with $\sim \ln(N)$ steps, and even small correlations could quickly span the system. One might expect that there would be a crossover between the average connectivity and $\ln(N)$ separating broadly distributed avalanches from localized ones, which would be very weak. Hence, HO might still work reasonably well in those systems down to low connectivities for most practical system sizes. In fact, our preliminary studies of Gaussian spin glasses on 3-connected graphs showed only minor deterioration in HO compared to EO for increasing system sizes (up to $N = 1023$). Yet, an independent comparison of HO to itself within a one-parameter family of models in the spirit of our approach here would require much more simulation for variable connectivity.

These results also highlight one important ingredient for any efficient algorithm or heuristic: the ability to travel between very distant regions of configuration space without being impaired by the large energy barriers that make such jumps energetically or entropically unfavorable. This ability is only within HOs reach for Infinitely Range systems.

V. ACKNOWLEDGMENTS

We would like to thank Helmut Katzgraber for inspiring discussions and the Division of Materials Research at the NSF for their support under grant #0312150 and the Emory University Research Council for seed funding.

-
- [1] A. Hartmann and H. Rieger, editors. *New Optimization Algorithms in Physics*. Springer, Berlin, 2004.
 - [2] H. Frauenfelder, editor. *Landscape Paradigms in Physics and Biology*. Elsevier, Amsterdam, 1997.
 - [3] D. J. Wales. *Energy landscapes*. Cambridge University Press, Cambridge, 2003.
 - [4] G. Zarand, F. Pazmandi, K.F. Pal, and G.T. Zimanyi. Using hysteresis for optimization. *Phys. Rev. Lett.*, 89:150201, 2002.
 - [5] K. F. Pal. Hysteretic optimization for the traveling salesman problem. *Physica A*, 329:287–297, 2003.
 - [6] K. F. Pal. Hysteretic optimization, faster and simpler. *Physica A*, 359:650–658, 2006.
 - [7] K. F. Pal. Hysteretic optimization for the Sherrington-Kirkpatrick spin glass. *Physica A*, 367:261–268, 2006.
 - [8] S. Kirkpatrick, C. D. Gelatt, and M. P. Vecchi. Optimization by simulated annealing. *Science*, 220:671–680, 1983.
 - [9] S. Boettcher and A. G. Percus. Optimization with extremal dynamics. *Phys. Rev. Lett.*, 86:5211–5214, 2001.
 - [10] D. Sherrington and S. Kirkpatrick. Solvable model of a spin-glass. *Phys. Rev. Lett.*, 35:1792–1796, 1975.
 - [11] S. F. Edwards and P. W. Anderson. Theory of spin glasses. *J. Phys. F: Metal Phys.*, 5:965, 1975.
 - [12] S. Zapperi, F. Colaiori, L. Dante, V. Basso, G. Durin, A. Magni, and M. J. Alava. Is demagnetization an efficient optimization method? *J. Magn. Mat.*, E1009:272–276, 2004.
 - [13] A.G. Percus, G. Istrate, and C. Moore. *Computational Complexity and Statistical Physics*. Oxford University Press, New York, 2006.
 - [14] G. Kotliar, P. W. Anderson, and D. L. Stein. One-dimensional spin-glass model with long-range random interactions. *Phys. Rev. B*, 27:R602, 1983.
 - [15] D. S. Fisher and D. A. Huse. Ordered phase of short-range ising spin-glasses. *Phys. Rev. Lett.*, 56:1601, 1985.
 - [16] D. S. Fisher and D. A. Huse. Equilibrium behavior of the spin-glass ordered phase. *Phys. Rev. B*, 38:386, 1988.
 - [17] H. G. Katzgraber and A. P. Young. Monte carlo studies of the one-dimensional ising spin glass with power-law interactions. *Phys. Rev. B*, 67:134410, 2003.
 - [18] H. G. Katzgraber and A. P. Young. Probing the almeida-thouless line away from the mean-field model. *Phys. Rev. B*, 72:184416, 2005.
 - [19] F. Pázmándi, G. Zaránd, and G. T. Zimányi. Self-organized criticality in the hysteresis of the Sherrington-Kirkpatrick model. *Phys. Rev. Lett.*, 83:1034–1037, 1999.
 - [20] H. H. Hoos and T. Stützle. *Stochastic Local Search: Foundations and Applications*. Morgan Kaufmann, San Francisco, 2004.
 - [21] P. Salamon, P. Sibani, and R. Frost. *Facts, Conjectures, and Improvements for Simulated Annealing*. Society for Industrial & Applied Mathematics, 2002.
 - [22] E. Marinari and G. Parisi. Simulated tempering: a new monte carlo scheme. *Europhys. Lett.*, 19:451–458, 1992.
 - [23] K. F. Pal. Hysteretic optimization, faster and simpler. *Physica A*, 360:525, 2006.
 - [24] A. J. Bray, M. A. Moore, and A. P. Young. Lower critical dimension of metallic vector spin-glasses. *Phys. Rev. Lett.*, 56:2641–2644, 1986.
 - [25] D. S. Fisher and D. A. Huse. Equilibrium behavior of the spin-glass ordered phase. *Phys. Rev. B*, 38:386–411, 1988.
 - [26] S. Boettcher and A. G. Percus. Nature’s way of optimizing. *Artificial Intelligence*, 119:275, 2000.
 - [27] S. Boettcher. Extremal optimization for sherrington-kirkpatrick spin glasses. *Euro. Phys. J. B*, 46:501, 2005.
 - [28] L. Viana and A. J. Bray. Phase diagrams for dilute spin-glasses. *J. Phys. C: Solid State Phys.*, 18:3037, 1985.